Environmental Resources Research
Vol. 8, No. 2, 2020

GUASNR

Characterizing soil infiltration parameters using field/laboratory measured and remotely-sensed data

M. Rahmati[1*], M.R. Neyshabouri[2], M. Mohammadi-Oskooei[3], A. Fakheri-Fard[4], A. Ahmadi[5]

[1]Associate Professor, Department of Soil Science and Engineering, Faculty of Agriculture, University of Maragheh, Maragheh, Iran.
[2]Professor, Department of Soil Science, Faculty of Agriculture, University of Tabriz, Tabriz, Iran
[3]Professor, Faculty of Mining Engineering, Sahand University of Technology, Tabriz, Iran
[4]Professor, Department of Water Engineering, Faculty of Agriculture, University of Tabriz, Tabriz, Iran
[5]Assistant Professor, Department of Water Engineering, Faculty of Agriculture, University of Tabriz, Tabriz, Iran

Received: August 2019; Accepted: May 2020

Abstract

Characterizing soil infiltration parameters is time consuming and costly. We carried out the current research to predict different parameters of soil infiltration using field/laboratory measured and remotely-sensed data. The investigated parameters included infiltration rates at different time intervals and the parameters of the three well-known infiltration models. We employed soil sampling and field measurements on late spring 2012 and acquired ETM+ data for the correspondent dates. We measured several soil properties as well as infiltration. Then, we developed several pedo-transfer functions (PTFs) from the collected field/laboratory measured and remotely sensed data to predict the intended infiltration parameters. Results showed that field/laboratory measured data were able to predict soil infiltration rates and parameters of the investigated models with reasonably high accuracies (E value up to 0.961). The results also revealed that, although there was no significant and robust relationship between soil surface reflectance and the investigated parameters, the developed PTFs had reasonable accuracies (E value up to 0.634) in estimating the intended infiltration parameters using soil characteristics (moisture content, soil separates, and organic carbon) which are predictable from remotely sensed data.

Keywords: Lighvan watershed, Remote sensing, Soil infiltration, Pedo-transfer functions

Introduction

Soil infiltration refers to water percolation downward from soil surface. Infiltration rate decreases nonlinearly through time and attains to a relatively constant value. Richards's Equation describes the phenomenon in the case of clearly defined and determined relationship between soil matric potential and hydraulic conductivity. Integration of Darcy's low and the continuity equation results in a general equation for the unsaturated soil water flow. In order to use this general equation to calculate the infiltration rate, user will need to determine soil moisture and matric potential as a function of time and soil depth. Clemmens (1983) believes that we need to simplify theoretical equations using several assumptions in order to make them applicable for soil infiltration rate predictions. However, even simplified forms are not applicable most of the time. Therefore, several mathematical equations or models have been introduced based on empirical data and are usually used to characterize soil infiltration process both in quantitative and qualitative points of views (Clemmens 1983). A single empirical equation is not also able to describe soil infiltration individually in different soils and different boundary conditions due to infiltration complicated process. Therefore, different researchers have introduced several models to simulate infiltration process. These empirical equations are site-

*Corresponding author; mehdirmti@gmail.com

specific and usually require calibration-using field measured infiltration data.

Different approaches have been applied for direct and basin measurements of soil infiltration (Mao et al., 2008). Direct methods are usually more appropriate in small regions. In contrast, basin methods are more suitable to measure soil infiltration at watershed scale. Basin methods use rainfall and runoff intensities of a single rainfall event to determine infiltration rate or cumulative infiltration (Mao et al., 2008). On the other hand, several methods including double rings, single ring, Marriott-double ring, disc infiltrometer, run off-on-ponding, run off-on-out, and linear source methods (Mao et al. 2008) also have been introduced for direct measurement of soil infiltration at local scales. Double rings method is the most conventional method to determine soil infiltration, which is of course time consuming and requires large volume of water to run it.

Pedo-transfer functions (PTFs) are of the mainly used approaches to link different soil characteristics (non-readily available ones) to the readily available data. Since soil hydraulic characteristics are the "hard to get and expensive" properties, soil scientists have applied PTFs to predict them using several readily available soil attributes. Bouma (1989) stated that PTFs are tools which convert available data to the needed ones. Several researchers have applied PTFs to estimate different soil properties including soil infiltration. For example, Mahdian et al. (2009) employed several linear and nonlinear regression functions between field/laboratory measured infiltration data and different soil characteristics including soil separates, bulk density, and soil moisture contents at field capacity (FC) and permanent wilting point (PWP). Their results revealed that although most of the developed PTFs were statistically significant but none of them resulted in reasonably robust correlations between measured and the predicted values. They subjected this to its complicated process and extensive controlling factors. They also suggested taking into account an appropriate indicator linking soil structure to its infiltration process. Sarmadian and Taghizadeh-Mehrjardi (2014) employing multiple linear regression and artificial neural network (ANN) model developed several PTFs to predict infiltration rate and deep percolation water. Their results showed that both ANN and regression methods predicted the investigated parameters with relatively high accuracies. Kashi et al. (2014) also employed several intelligence-based models including artificial neural networks (MLP and RBF), adaptive neuro-fuzzy inference system (ANFIS), and multiple regression (MR) techniques to develop several PTFs to predict infiltration rate. They reported that the MLP model predicted infiltration rate much better than ANFIS, MR, and RBF models. More recently, Rahmati (2017) also used multiple regression, artificial neural network, and group method of data handling in a competitive way to develop several PTFs to predict soil infiltration rates point-basely from several soil characteristics with relatively high accuracy with Nash-Sutcliffe value up to 0.963.

Availability of the input data is one of the important components of PTFs development. Satellite images are of the most highly concentrated multidisciplinary sources of the readily available data in earth surface investigations, which most of scientists as well as soil scientists are interested in. Soil scientists have mainly used remote sensing data to predict surface soil parameters including surface soil moisture (Rahmati et al., 2015, He et al., 2016), organic carbon (Ayoubi et al., 2011; Rahmati et al., 2016), evaporation rate (Bastiaanssen et al. 1998), surface albedo (Parviz et al., 2010), soil erosion (De Roo et al. 1996), soil salinity (Gorji et al. 2015, Scudiero et al. 2015, Rahmati and Hamzehpour, 2017) and so forth. Although there is no report, up to our knowledge, on remote sensing data usages to predict surface soil infiltration yet, it seems that establishment of a logical relation between remotely sensed data and soil infiltration rate or parameters of infiltration models can be an effective step in terms of time and cost. However, direct prediction of infiltration rate or its parameters using remotely sensed data (soil surface

reflectance or radiations) sounds very complicated. Therefore, employing empirical relationships between soil infiltration parameters and its surface characteristics (such as soil moisture, organic carbon, soil texture, soil salinity, slope, etc.), which are predictable using remotely sensed data seems to be more valuable and applicable approach at this time. Furthermore, some promising results in remote sensing of runoff (Guo et al., 2011) lead to optimism in remote sensing of soil infiltration. Therefore, in the current research, we intended to link different hydraulic characteristics of surface soil including infiltration rates and the parameters of Green and Ampt (GAM), Kostiakov (KM), and modified Kostiakov (MKM) models to field or laboratory measured data as well as remotely sensed ones.

Materials and Methods

Study Area

We conducted this study at Lighvan Watershed, East Azerbaijan, located in North Western Iran, between latitudes 37° 43' 07" to 37° 50' 08" N and longitudes 46° 22' 23" to 46° 28' 05" E. The watershed has an area of 7,854 hectares and an elevation varying from 3,534m in uplands to 2,190m in the watershed outlet (Figure 1), with an average rainfall of 320 mm per year. Bare lands (46%) and poor pasture (42%) comprise the major parts of the study area (Figure 1) (Rahmati et al., 2015), while only 12% of the area is covered by irrigated and rainfed farming (Rahmati et al., 2015). As seen from Figure 2, most parts of the study area (65%) have aspect of east, northeast and northwest as well as north.

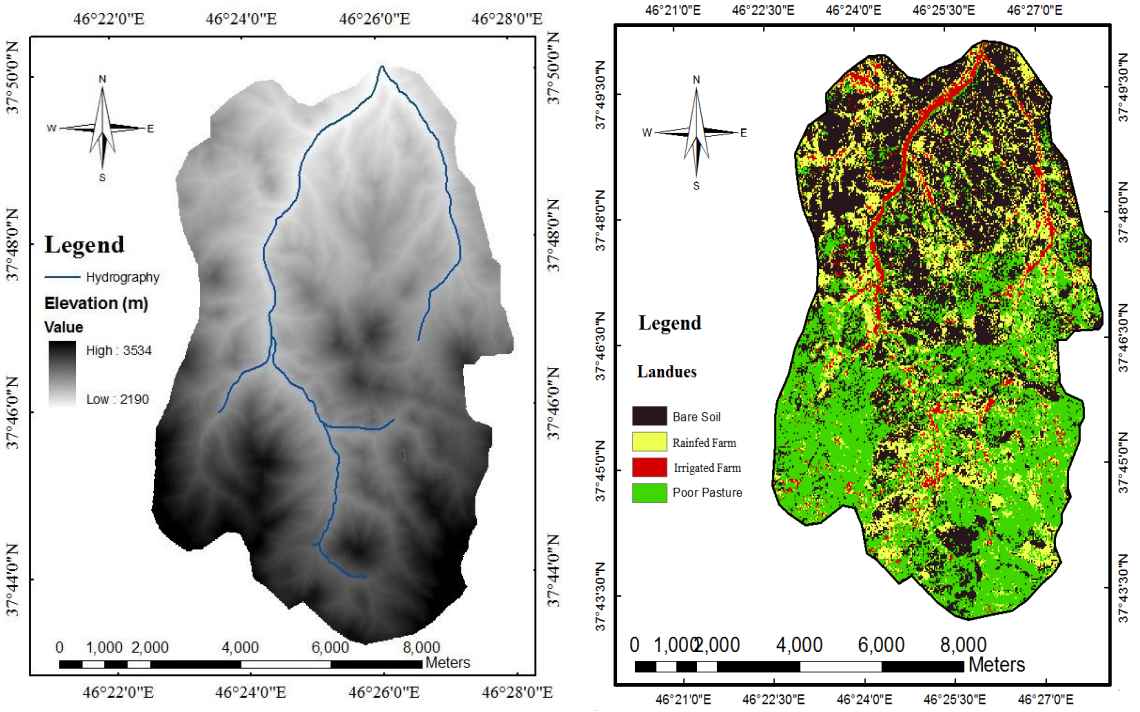

Figure 1. DEM (left) and land use (right) maps of the Lighvan Watershed, located in northwest of Iran

Soil sampling

Prior to soil sampling, we divided the study area into 1-hectare square pixels and then took soil samples from each pixel in order to employ a randomized controlled sampling strategy. From 45 cells and five soil samples per cell, we collected 225 samples from 0-15 cm depths on late spring 2012. Samples locations were recorded using handheld Garmin GPS and then were registered in ArcGIS for further use.

Laboratory measurements

Using soil samples, we determined soil textures through hydrometer method (Gee

and Or 2002), soil organic carbon through wet oxidation (Nelson and Sommers 1982), soil aggregate stability (*WAS*) through wet-sieving (Nimmo and Perkins, 2002), and soil electrical conductivity (*EC*) in paste saturation extracts through EC-meter. In order to measure soil moisture content, we repeated soil sampling on two different days (11-June-2012 and 18-June-2012). We applied the first day's data to calibrate the polynomials developed for the soil moisture content prediction from the remote sensing data and the second day's data for their validation. No rainfall occurred during the period 11-June until 18-June 2012, between two sampling dates.

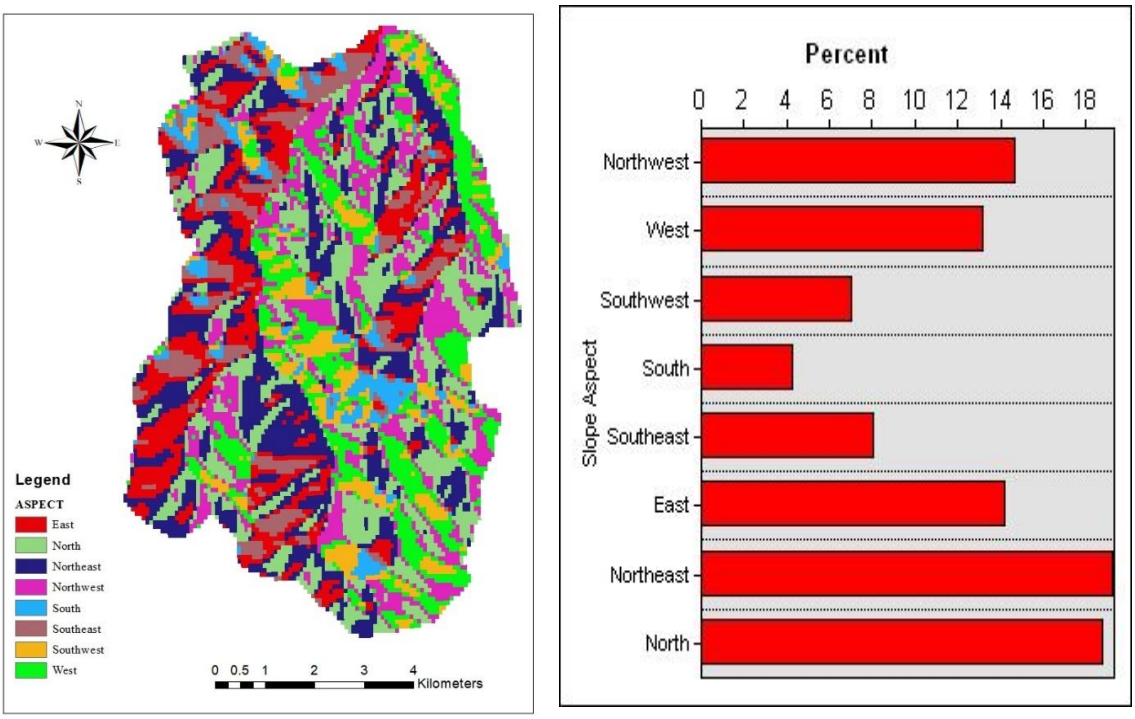

Figure 2. Map of the aspects in Lighvan Watershed (left) and their percentage (right)

Furthermore, a number of 135 undisturbed soil samples taken from the study area (3 samples per cell) were employed to determine saturated hydraulic conductivity by falling head method (Reynolds et al., 2002), bulk density (Grossman and Reinsch, 2002), and saturated moisture content by volumetric method (Dane and Hopmans, 2002). Soil infiltration was measured at the sampling locations using disc infiltrometer (Perroux and White 1988). For this, the suction head was set to zero and the measurements continued for 45 minutes.

Satellite images

We used images from ETM+ sensor of Landsat 7 dated 13-Jun-2012, 15-July-2012, and 17-Sep-2012 to fulfil the current research. The spatial, spectral, and temporal resolutions of the ETM+ data are 15 and 30 meters, 8 bands, and 16 days, respectively. We acquired ETM+ data for sampling dates through USGS website. We applied all needed pre-processing steps on the remote sensing data to obtain accurate calculations. Georeferencing and atmospheric correction were the only corrections needed in our project. No geometric correction was needed for our data.

Input and output variables in PTFs development

We applied four sets of data to develop PTFs for predicting soil infiltration parameters. The first set included clay (*CC*), silt (*Si*), and sand (*Sa*) percent, saturated hydraulic conductivity (K_s), bulk (D_b) and particle (D_p) densities, wet-aggregate stability (*WAS*), antecedent (θ_i)

and field saturated (θ_{fs}) moisture contents, organic carbon (*OC*), and electrical conductivity (*EC*) of saturated paste as input variables and soil infiltration parameters as output. The second data set comprised remotely sensed data as input variables to predict infiltration parameters including soil infiltration rates at different time intervals and parameters of GAM, KM, and MKM models. In this regard, we used soil surface reflectance from different bands of ETM+ data (Band1 to Band5, Band6_1, and Band6_2) as independent variables. The third data set considered both ground measured (*CC*, *Si*, *Sa*, K_s, D_b, D_p, *WAS*, θ_i, θ_{fs}, *OC*, and *EC*) and remotely sensed (Band1 to Band5, Band6_1, and Band6_2) data as input variables to predict soil infiltration parameters.

We decided to use only the ground measured data, which are potentially predictable from remotely sensed data in order to provide an indirect method to estimate soil infiltration parameters through remotely sensed data. To this end, we chose soil moisture content, soil texture, soil organic carbon, and soil salinity as independent variables because previously published results of the same watershed revealed the applicability of the remotely sensed data to predict these variables. The details for applicability of remotely sensed data to predict the selected properties are reported by Rahmati (2016) and Rahmati et al. (2014, 2015, 2016) and will not be outlined here. The main purpose of the current article is to focus on the feasibility of remote sensing for prediction and mapping of the soil infiltration and its parameters.

We intended to model the parameters of GAM, KM, and MKM models because the previously published results (Rahmati et al. 2016) revealed that these models showed the best conformity with the measured infiltration data compared to other applied models including Horton and Philip's two- and three terms models. We aimed at development of PTFs to provide an easy and fast method to predict the parameters of the three selected models using soil readily available data.

PTFs development methodology

To develop PTFs, we employed the following steps in a consecutive order:

1- All input and output variables were normalized to assign data between zero and 1 using the following formula:

$$Z_i = \frac{X_i - X_{\min}}{X_{\max} - X_{\min}} \quad (1)$$

2- Applying all data sets outlined above, we evaluated the Pearson correlation coefficients between input variables and the investigated parameters including infiltration rates at different time intervals and parameters of GAM (K_a and b), KM (α and b), and MKM (α, b, and c) models to find out the most important and significant predictors in PTFs development. We selected only those input variables with significant correlations for the next step.

3- Using selected predictors from previous step, we applied three types of polynomials including first, second, and third order polynomials to develop PTFs to predict the investigated parameters. The general forms of the applied polynomials were as follows:

$$1^{st}\text{ order:}\quad \text{Target} = \sum_{i=1\text{ to }n}^{j=0:1} a_{ji} Input_i^j \quad (2)$$

$$2^{nd}\text{ order:}\quad \text{Target} = \sum_{i=1\text{ to }n}^{j=0,1\text{ and }2} a_{ji} Input_i^j \quad (3)$$

$$3^{rd}\text{ order:}\quad \text{Target} = \sum_{i=1\text{ to }n}^{j=0,1,2,\text{ and}3} a_{ji} Input_i^j \quad (4)$$

PTFs evaluations

In order to evaluate PTFs, we split data sets into two groups of training (75%) and test (25%). We used the training data to develop PTFs and the test data were used to evaluate results in an independent manner. We evaluated PTFs' accuracy applying root mean square error (RMSE), evaluation error (ER), and Nash-Sutcliffe (E) criteria between measured and predicted values:

$$RMSE = \sqrt{\frac{\sum(\log X_m - \log X_p)\text{^}2}{n}} \quad (5)$$

$$ER = \frac{RMSE}{\overline{X_m}} \times 100 \quad (6)$$

$$E = 1 - \frac{\sum(X_m - X_p)^2}{\sum(X_m - \overline{X_m})^2} \quad (7)$$

where, X_m and X_p are measured and predicted saturated hydraulic conductivities, respectively with mean value of $\overline{X_m}$ for measured one. A value of RMSE near zero denotes a better accuracy of the method. ER tries to present the standardized RMSE error in percent with lower values of ER implying better accuracy and vice versa. The E has a range [–∞, 1]; E = 1 shows a perfect match; E = 0 means that the average of observed values is as good as predicted values; for E <0, the model is worse for prediction than taking only the mean of the observed values; E >0.9 shows that the slope between observed and predicted values is near unity.

Results

Table 1 reports statistical description of the measured soil properties. Nearly all parts of the study area have coarse textured soils consisting of sandy loam, loam, sandy clay loam, and sand texture classes. Table 2 reports statistical parameters of the measured initial and final infiltration rates in the study area as well as antecedent and field saturated soil moisture contents. We considered the soil infiltration rate at first step (first 30-second) as initial soil infiltration rate.

Table 1. Statistical parameters of measured features in the current study

Parameters		Maximum	Minimum	Mean	*CV* (%)
Texture*	Clay (%)	38.83	5.35	17.36	32.66
	Silt (%)	48.01	6.21	25.56	26.66
	Sand (%)	84.68	33.59	56.08	16.87
Aggregate stability* (%)		95.92	25.14	65.37	27.51
Saturated hydraulic conductivity** (cm/h)		48.60	1.03	6.68	79.19
Bulk density** (g/cm^3)		1.49	1.20	1.35	3.70
Particle density** (g/cm^3)		2.65	2.21	2.48	4.44
Organic carbon* (%)		2.05	0.10	0.85	45.88
Electrical conductivity* (mS/cm)		1.20	0.30	0.69	37.68
Moisture content* (cm^3/cm^3)	Step 1	0.287	0.105	0.169	18.93
	Step 2	0.264	0.087	0.150	20.67

*: measured in 225 disturbed soil samples; **: measured in 135 undisturbed soil samples, CV: coefficient variation

Table 2. Statistical description of infiltration rate and antecedent and field saturated moisture contents in the study area

Parameter	Minimum	Maximum	Mean	Coefficient variation (%)
Initial infiltration rate (cm/h)	2.23	33.48	13.15	50.72
Final infiltration rate (cm/h)	0.391	7.65	2.59	61.00
Antecedent moisture content (%)	0.04	0.29	0.14	42.86
Field saturated moisture content (%)	0.33	0.54	0.44	11.36

Tables 3 to 6 report simple Pearson correlation coefficients (R) between ground measured and remotely sensed data and investigated parameters. Table 3 reveals that nearly all ground measured data excluding EC, OC, and D_p had significant correlations with infiltration rates at different time intervals. The OC and D_p were also significantly correlated with infiltration rates at higher time intervals. Among the ground-measured data, K_s had the highest correlations with infiltration rates with R value between 0.811 and 0.977 while θ_i and CC ranked second and both negatively correlated with infiltration rates showing R value between -0.476 and -0.645. Sa, D_b, θ_{fs}, WAS, and Si are the other parameters which were significantly correlated with infiltration rates at different time intervals.

Table 4, reporting R value between ground measured data and parameters of GAM (K_a and b), KM (α and b), and MKM (α, b, and i_c) models, shows that parameter i_c of MKM model had the highest significant correlation with K_s scoring R at 0.977. The correlations between parameter K_a of GAM, parameter a of KM and MKM with the respective R values of 0.917, 0.958, and 0.735 ranked the third.

Tables 5 and 6 report R values between the investigated parameters and soil surface reflectance of different bands of ETM+ data. The tables report no significant correlations with the exception of Band4. Band4 of ETM+ showed significant correlations with infiltration rates at time intervals 0.5 to 8 minutes as well as parameters of the investigated infiltration models. Although the obtained R value between Band4 of ETM+ and the investigated parameters were low (around -0.2), the existence of significant correlation between remotely sensed data and infiltration parameters brings hope for further investigations.

Table 3. Pearson correlation coefficient (*R*) between soil readily available data and infiltration rates at different time intervals (n=134)

Parameter±		K_s	D_b	θ_{fs}	θ_i	*WAS*	*CC*	*Si*	*Sa*	*OC*	D_p	*EC*
Infiltration rate (cm/h)	0.5	0.857	-0.385	0.314	-0.545	0.128	-0.634	-0.248	0.542	0.090	-0.144	-0.051
	1	0.848	-0.362	0.302	-0.539	0.159	-0.619	-0.230	0.520	0.092	-0.142	-0.008
	1.5	0.833	-0.334	0.289	-0.493	0.174	-0.611	-0.231	0.517	0.124	-0.167	0.038
	2	0.834	-0.332	0.274	-0.492	0.176	-0.625	-0.222	0.518	0.115	-0.159	0.027
	2.5	0.832	-0.334	0.284	-0.520	0.189	-0.608	-0.209	0.499	0.089	-0.117	0.041
	3	0.833	-0.320	0.298	-0.538	0.206	-0.599	-0.186	0.476	0.074	-0.105	0.042
	3.5	0.812	-0.362	0.277	-0.487	0.212	-0.632	-0.159	0.474	0.085	-0.124	0.040
	4	0.811	-0.390	0.255	-0.476	0.202	-0.643	-0.146	0.470	0.103	-0.147	0.034
	6	0.926	-0.326	0.326	-0.602	0.216	-0.545	-0.162	0.429	0.164	-0.229	0.058
	8	0.937	-0.336	0.324	-0.639	0.215	-0.534	-0.172	0.429	0.148	-0.209	0.050
	10	0.946	-0.360	0.322	-0.645	0.210	-0.537	-0.162	0.423	0.148	-0.224	0.047
	15	0.971	-0.381	0.379	-0.621	0.197	-0.530	-0.176	0.429	0.176	-0.230	0.012
	20	0.973	-0.382	0.390	-0.628	0.192	-0.527	-0.177	0.429	0.169	-0.222	0.008
	25	0.974	-0.384	0.379	-0.631	0.195	-0.528	-0.174	0.427	0.170	-0.227	0.005
	30	0.972	-0.392	0.394	-0.622	0.204	-0.522	-0.175	0.425	0.182	-0.237	0.003
	35	0.976	-0.401	0.405	-0.614	0.194	-0.531	-0.174	0.429	0.189	-0.243	-0.006
	40	0.977	-0.400	0.406	-0.606	0.196	-0.519	-0.173	0.421	0.194	-0.246	-0.002
	45	0.977	-0.396	0.416	-0.602	0.195	-0.514	-0.177	0.422	0.189	-0.246	-0.009

±: All reported correlations were significant at P < 0.05 probability level excluding underlined ones
K_s in cm/h, D_b and D_p in g/cm^3, θ_i and θ_{fs} in cm^3/cm^3, *WAS* and *OC* in %, *CC*, *Si*, and *Sa* in g/g, and *EC* in dS/m

Table 4. Pearson correlation coefficient (*R*) between soil available data and parameters of GAM, KM, and MKM models (n=134)

Parameter±	GAM $i = K_a + b/I$		KM $I = at^b$		MKM $I = at^b + i_c t$		
	K_a	*b*	*a*	*b*	i_c	*a*	*b*
K_s	0.917	0.791	0.958	0.373	0.977	0.735	0.044
D_b	-0.333	-0.298	-0.376	-0.034	-0.396	-0.268	0.107
θ_{fs}	0.328	0.304	0.355	0.223	0.416	0.168	-0.287
θ_i	-0.568	-0.490	-0.613	-0.187	-0.602	-0.516	-0.128
WAS	0.250	0.134	0.212	0.187	0.195	0.187	0.214
CC	-0.542	-0.507	-0.572	0.136	-0.514	-0.592	-0.051
Si	-0.141	-0.261	-0.178	0.018	-0.177	-0.164	0.031
Sa	0.410	0.481	0.455	-0.091	0.422	0.456	0.005
OC	0.166	0.133	0.156	0.228	0.189	0.057	0.063
D_p	-0.207	-0.196	-0.211	-0.246	-0.246	-0.097	-0.080
EC	0.088	-0.050	0.034	0.066	-0.009	0.092	0.230

±: All reported correlations were significant at P < 0.05 probability level excluding underlined ones
K_s in cm/h, D_b and D_p in g/cm^3, θ_i and θ_{fs} in cm^3/cm^3, *WAS* and *OC* in %, *CC*, *Si*, and *Sa* in g/g, and *EC* in dS/m

Table 5. Pearson correlation coefficient (R) between soil surface reflectance of ETM+ bands and infiltration rates at different time intervals (n=134)

Parameter±		Band1	Band2	Band3	Band4	Band5	Band61	Band62
Infiltration rates (cm/h)	0.5	-0.078	-0.054	-0.023	-0.202	-0.052	0.065	0.066
	1	-0.093	-0.072	-0.038	-0.220	-0.069	0.053	0.054
	1.5	-0.119	-0.103	-0.066	-0.267	-0.087	0.028	0.031
	2	-0.116	-0.101	-0.062	-0.277	-0.082	0.039	0.040
	2.5	-0.109	-0.091	-0.054	-0.259	-0.065	0.046	0.047
	3	-0.076	-0.065	-0.026	-0.262	-0.047	0.065	0.066
	3.5	-0.073	-0.062	-0.023	-0.246	-0.045	0.095	0.096
	4	-0.071	-0.061	-0.028	-0.252	-0.070	0.084	0.084
	6	-0.044	-0.041	-0.025	-0.199	-0.077	0.048	0.052
	8	-0.003	-0.004	0.008	-0.180	-0.062	0.073	0.076
	10	0.001	0.000	0.009	-0.169	-0.064	0.077	0.081
	15	-0.010	-0.006	0.005	-0.153	-0.052	0.041	0.045
	20	-0.008	-0.005	0.004	-0.144	-0.048	0.043	0.046
	25	-0.007	-0.004	0.004	-0.139	-0.048	0.038	0.041
	30	-0.005	-0.002	0.007	-0.131	-0.042	0.044	0.048
	35	0.002	0.007	0.015	-0.122	-0.038	0.042	0.046
	40	-0.007	-0.002	0.007	-0.121	-0.037	0.034	0.038
	45	-0.007	0.000	0.007	-0.117	-0.033	0.032	0.036

±: Only underlined correlations were significant at P < 0.05 probability level

Table 6. Pearson correlation coefficient (R) between soil surface reflectance of ETM+ bands and parameters of different infiltration models (n=134)

Parameter±	GAM $i = K_a + b/I$		KM $I = at^b$		MKM $I = at^b + i_c t$		
	K_a	b	a	b	i_c	a	b
Band1	-0.044	-0.103	-0.032	0.156	-0.007	-0.086	0.024
Band2	-0.046	-0.077	-0.027	0.116	0.000	-0.082	-0.018
Band3	-0.024	-0.046	-0.009	0.083	0.007	-0.045	0.003
Band4	-0.226	-0.212	-0.189	0.031	-0.117	-0.299	-0.320
Band5	-0.068	-0.045	-0.059	0.073	-0.033	-0.102	-0.076
Band61	0.043	0.038	0.055	-0.048	0.032	0.087	0.062
Band62	0.046	0.039	0.058	-0.042	0.036	0.087	0.059

±: Only underlined correlations were significant at P < 0.05 probability level

Applying regression analysis, we developed three polynomials with first to third orders between the investigated parameters (soil infiltration rates at different time intervals (18-time intervals) and parameters of GAM, KM, and MKM models) and ground-measured data.

Applying second and third order polynomials resulted in very slight improvement in PTFs accuracy (with average E 0.796 for the first order polynomial *vs*. 0.813 and 0.827 for the second and third orders, respectively). However, they comprise higher numbers of coefficients, which make their use more complicated. Therefore, the results for second and third order polynomials are not outlined here. Table 7 reports the accuracy for the developed PTFs through training, test, and complete datasets. Since the

number of developed PTFs is high (25 equations), we decided to report the PTFs coefficients only (Table 8).

According to Table 7, the developed PTFs offer higher accuracies to predict infiltration rates at different time intervals showing E between 0.719 and 0.964 for the training dataset, 0.553 to 0.965 for the test data set, and 0.727 to 0.960 for the complete dataset. In addition to PTFs for infiltration rates, we developed several other PTFs to predict the parameters of the investigated infiltration models. The developed PTFs led to accurate predictions of parameter i_c of GAM, parameter *a* of KM, and parameter i_c of MKM with E higher than 0.783 for the training, test, and all data sets. However, they showed very low accuracies for predictions of the parameter b of KM, and parameter *a* of MKM with E being lower than 0.264.

Table 7. The accuracy of developed PTFs to predict the investigated parameters using ground measured data (n=134)

Parameter		Train			Test			All data		
		RMSE	ER	E	RMSE	ER	E	RMSE	ER	E
Infiltration rates	0.5	0.089	25.25	0.804	0.114	34.90	0.774	0.096	27.66	0.795
	1	0.095	29.01	0.775	0.090	27.77	0.792	0.094	28.71	0.779
	1.5	0.093	30.89	0.752	0.100	39.29	0.729	0.095	32.74	0.748
	2	0.122	31.23	0.759	0.125	34.35	0.757	0.122	31.96	0.759
	2.5	0.124	35.49	0.731	0.109	26.79	0.783	0.120	33.14	0.746
	3	0.114	31.47	0.781	0.131	42.21	0.590	0.119	33.89	0.747
	3.5	0.115	32.63	0.760	0.121	33.01	0.553	0.117	32.73	0.727
	4	0.110	33.06	0.719	0.108	33.77	0.754	0.109	33.23	0.728
	6	0.057	23.95	0.869	0.067	24.52	0.907	0.060	24.17	0.885
	8	0.055	21.22	0.911	0.071	21.10	0.901	0.059	21.34	0.910
	10	0.053	19.19	0.923	0.050	20.49	0.925	0.052	19.49	0.924
	15	0.043	13.79	0.954	0.054	18.63	0.949	0.046	14.98	0.953
	20	0.041	14.84	0.949	0.052	14.37	0.962	0.044	14.79	0.956
	25	0.040	14.12	0.961	0.048	14.84	0.955	0.042	14.37	0.960
	30	0.041	14.43	0.962	0.053	18.11	0.914	0.045	15.45	0.952
	35	0.042	13.81	0.964	0.052	14.61	0.948	0.044	14.10	0.960
	40	0.043	14.16	0.957	0.048	15.56	0.963	0.045	14.52	0.959
	45	0.042	14.23	0.957	0.048	14.88	0.965	0.043	14.43	0.960
GAM	i_c	0.072	22.28	0.885	0.096	24.75	0.783	0.078	23.18	0.863
	b	0.097	54.66	0.626	0.108	47.37	0.712	0.100	52.56	0.661
KM	*a*	0.049	15.25	0.948	0.061	22.32	0.884	0.052	16.85	0.937
	b	0.147	29.82	0.222	0.160	30.85	-0.099	0.150	30.11	0.157
MKM	*a*	0.122	37.23	0.696	0.162	39.89	0.370	0.133	38.31	0.634
	b	0.167	27.26	0.264	0.204	31.85	-0.074	0.177	28.55	0.183
	i_c	0.043	13.89	0.958	0.043	15.72	0.967	0.043	14.30	0.961
	Mean	0.081	24.53	0.803	0.091	26.48	0.747	0.083	25.02	0.794

Table 8. Coefficients of developed polynomials (PTFs) to predict the investigated parameters using ground measured data

Parameter		Intercept	K_s	D_b	θ_{fs}	θ_i	*WAS*	*CC*	*Si*	*Sa*	*OC*	D_p	*EC*
Infiltration rates	0.5	-14.536	0.659	-0.033	0.024	-0.004	-	7.843	11.57	12.898	-	-	-
	1	-16.018	0.585	0.067	0.041	-0.063	-	8.593	12.76	14.154	-	-	-
	1.5	-1.724	0.586	0.152	0.009	-0.081	0.040	0.794	1.39	1.686	-	-	-
	2	-0.542	0.740	0.122	-0.061	-0.068	0.053	0.107	0.57	0.739	-	-	-
	2.5	-7.400	0.772	0.125	-0.015	-0.082	0.086	3.893	5.88	6.626	-	-	-
	3	12.661	0.702	0.117	0.059	-0.131	0.072	-7.157	-9.80	-10.82	-	-	-
	3.5	0.235	0.630	0.062	0.042	-0.069	0.034	-0.374	-	0.050	-	-	-
	4	0.287	0.537	0.045	-0.001	-0.090	0.040	-0.360	-	0.020	-	-	-
	6	0.121	0.703	0.079	-0.040	-0.096	0.025	-0.126	-	-0.029	-	-0.007	-
	8	-3.298	0.752	0.100	-0.054	-0.119	0.054	1.730	2.67	2.940	-	0.023	-
	10	0.164	0.702	0.117	-0.036	-0.198	0.044	-0.112	-	-0.018	-	-0.021	-
	15	-6.385	0.828	0.058	0.005	-0.092	0.015	3.412	5.08	5.628	0.036	0.028	-
	20	-3.154	0.811	0.033	0.006	-0.122	0.027	1.697	2.57	2.835	-	0.011	-
	25	-3.492	0.829	0.067	0.019	-0.102	0.016	1.818	2.79	3.060	0.060	0.034	-
	30	-8.039	0.807	0.051	0.046	-0.098	0.016	4.337	6.39	7.055	0.024	-0.026	-
	35	-0.220	0.826	0.044	0.060	-0.139	0.014	0.030	0.27	0.265	0.063	0.008	-
	40	-6.544	0.870	0.023	0.045	-0.068	-0.008	3.526	5.19	5.719	0.057	0.015	-
	45	-3.889	0.916	0.072	0.033	-0.037	0.011	2.094	3.03	3.388	0.005	0.002	-
GAM	i_c	-0.004	0.932	0.197	-0.067	-0.059	0.074	-0.112	-	-0.036	-	0.075	-
	b	-7.103	0.484	0.084	0.005	-0.034	-	3.795	5.59	6.285	-	-0.022	-
KM	*a*	-11.379	0.789	0.095	-0.013	-0.128	0.032	6.148	9.09	10.005	-	-0.019	-
	b	0.350	0.248	-	0.055	-0.074	0.058	-	-	-	0.071	0.022	-
MKM	i_c	-8.678	0.883	0.029	0.049	-0.035	-0.006	4.678	6.83	7.547	0.043	0.024	-
	a	0.388	0.444	0.184	-	-0.252	0.086	-0.464	-	-0.038	-	-	-
	b	0.585	-	-	-0.326	-	0.259	-	-	-	-	-	0.152

In addition to ground-measured data, we also applied remotely sensed data from ETM+ images to predict the investigated parameters. For this, we evaluated the relationships between infiltration rates at different time intervals (0.5, 1, 1.5, 2… and 45 minutes) and soil surface reflectance of ETM+ bands to predict soil infiltration rate more directly using surface soil reflectance. Since we previously showed that only soil surface reflectance from Band 4 of ETM+ data had significant correlations with the investigated parameters, we were not able to develop strong PTFs for parameters predictions. Even second and third order polynomials did not result in better accuracies for parameters predictions. The best developed PTF had E 0.103 and the others were near zero showing that if we use the average value of the measured parameters, it would be as good as the predicted values by the developed PTFs. Therefore, we do not supply details for the results here.

We also intended to predict the investigated parameters using the soil properties which are predictable by remote sensing data. In this regard, the input variables were restricted to soil moisture content, soil separates, soil organic carbon, and soil salinity because previously published results of the same study area revealed the applicability of the remotely sensed data to predict these properties (Rahmati et al. 2014, 2015, 2016; Rahmati, 2016).

Table 9. The accuracy of developed PTFs to predict the investigated parameters indirectly using remotely sensed data (n=134)

Parameter		Training			Test			All data		
	Time	RMSE	ER	E	RMSE	ER	E	RMSE	ER	E
Infiltration rates	0.5	0.131	38.91	0.609	0.167	43.93	0.409	0.141	40.51	0.561
	1	0.133	42.08	0.608	0.148	41.17	0.021	0.137	41.88	0.530
	1.5	0.146	48.01	0.424	0.089	37.06	0.712	0.134	46.55	0.491
	2	0.180	45.87	0.500	0.159	45.09	0.515	0.175	45.75	0.506
	2.5	0.165	45.06	0.530	0.177	50.04	0.425	0.168	46.28	0.506
	3	0.175	50.63	0.409	0.134	36.32	0.739	0.165	47.20	0.510
	3.5	0.164	43.77	0.431	0.130	42.88	0.689	0.156	43.78	0.511
	4	0.151	45.28	0.481	0.128	40.66	0.626	0.146	44.30	0.517
	6	0.110	45.87	0.586	0.152	56.02	0.365	0.122	49.13	0.525
	8	0.132	47.10	0.537	0.127	47.29	0.625	0.131	47.15	0.561
	10	0.125	46.96	0.564	0.121	44.90	0.579	0.124	46.46	0.568
	15	0.127	39.34	0.641	0.136	51.63	0.574	0.129	41.93	0.631
	20	0.141	47.17	0.508	0.148	50.02	0.603	0.143	47.87	0.537
	25	0.118	43.65	0.620	0.151	41.73	0.625	0.127	43.33	0.634
	30	0.123	42.13	0.631	0.127	45.63	0.634	0.124	42.96	0.632
	35	0.124	38.08	0.692	0.166	58.31	0.419	0.135	42.99	0.629
	40	0.127	41.01	0.668	0.161	53.80	0.473	0.136	44.33	0.620
	45	0.137	42.87	0.616	0.130	54.24	0.521	0.135	45.12	0.608
GAM	i_c	0.141	44.46	0.542	0.128	44.24	0.618	0.138	44.45	0.562
	b	0.158	31.60	0.088	0.144	29.22	0.154	0.155	31.04	0.103
KM	*a*	0.159	47.09	0.435	0.120	35.66	0.676	0.150	44.55	0.494
	b	0.132	70.11	0.438	0.137	70.35	0.225	0.134	70.18	0.395
MKM	*a*	0.149	42.11	0.530	0.179	54.40	0.384	0.157	45.12	0.492
	b	0.185	29.36	0.042	0.207	35.42	0.027	0.191	30.80	0.049
	i_c	0.144	47.71	0.557	0.101	34.18	0.782	0.135	44.86	0.613
	Mean	0.143	44.25	0.507	0.143	45.77	0.497	0.144	44.74	0.511

Similar to previous steps, we applied the first to third order polynomials to develop PTFs for the parameters' predictions in this step, too. Since reporting all developed PTFs (75 equations) seems redundant, we initially compared the results to check if the second and third order polynomials had affected the accuracy of the PTFs. According to the results, the third order polynomial showed the best performance via training data set (with average E being 0.640) compared to the first and second order polynomials (with respective average E being 0.507 and 0.583). However, the performance of the first order polynomial was similar to or better than the second and third order polynomials via test data set (with average E 0.497 vs. 0.412 and 0.483). Therefore, we selected the first order polynomial for simplicity. Table 9 reports the accuracy of the developed PTFs (first order polynomial) to predict the investigated parameters. Table 10 reports the coefficients of the developed PTFs.

The results revealed that the developed PTFs led to relatively accurate predictions of infiltration rates at different time intervals with E values between 0.409 and 0.692 for the training data set, 0.409 and 0.712 for the test data set (excluding infiltration rate at time interval of one minute with E value of 0.021), and 0.491 to

0.634 for all data set. The results also revealed moderate accuracies for prediction of parameters of the investigated infiltration models. Based on the training data set, the developed PTFs showed E to be between 0.435 and 0.557 to predict parameters of the investigated infiltration models excluding parameter b of GAM (with E of 0.088) and parameter b of MKM (with E 0.042) models. According to the test data, the developed PTFs also consisted of moderately high accuracies showing E values between 0.384 and 0.782 excluding parameter b of GAM (with E = 0.154), KM (with E = 0.225), and MKM (with E of 0.027).

Table 10. Coefficients of developed polynomials (PTFs) to predict the investigated parameters using indirect remote sensing data

Parameter	time	Intercept	θ_i	*CC*	*Si*	*Sa*	*OC*	*EC*
Infiltration rates	0.5	2.307	-0.462	-1.378	-1.207	-1.258	-	-
	1	-7.556	-0.491	4.032	6.547	7.322	-	-
	1.5	-6.300	-0.356	3.370	5.444	6.100	-	-
	2	-3.468	-0.489	1.752	3.448	3.810	-	-
	2.5	12.419	-0.511	-6.963	-9.014	-10.048	-	-
	3	-4.416	-0.434	2.244	4.131	4.535	-	-
	3.5	0.837	-0.405	-0.611	-	-0.029	-	-
	4	0.759	-0.327	-0.628	-	-0.021	-	-
	6	0.734	-0.489	-0.431	-	-0.106	-	-
	8	-7.740	-0.541	4.197	6.725	7.349	-	-
	10	0.776	-0.533	-0.469	-	-0.068	-	-
	15	-2.497	-0.701	1.330	2.588	2.833	0.319	-
	20	-0.903	-0.546	0.428	1.381	1.430	-	-
	25	8.365	-0.589	-4.681	-5.979	-6.681	0.233	-
	30	10.391	-0.607	-5.807	-7.559	-8.451	0.286	-
	35	17.247	-0.697	-9.523	-12.939	-14.398	0.437	-
	40	-7.851	-0.661	4.176	6.832	7.414	0.330	-
	45	-1.432	-0.766	0.748	1.785	1.870	0.362	-
GAM	i_c	0.852	-0.496	-0.526	-	-0.074	-	-
	b	-13.461	-0.403	7.381	10.965	12.206	-	-
KM	*a*	3.492	-0.545	-1.979	-2.077	-2.360	-	-
	b	0.495	-	-	-	-0.138	-	0.216
MKM	i_c	2.151	-0.672	-1.262	-1.050	-1.275	0.336	-
	a	0.810	-0.463	-0.561	-	-	-	0.022
	b	0.570	-	-	-	-	-	0.135

Discussion

Determination of soil infiltration rate and its parameters are of the most time consuming, costly, and highly needed soil characteristics. Therefore, several researchers, e.g., Jemsi et al. (2013), Kashi et al. (2014), Sarmadian and Taghizadeh-Mehrjardi (2014), and Rahmati (2017), attempted to develop several PTFs to predict soil infiltration and its parameters using soil readily available characteristics. In this regard, we intended to develop several PTFs to predict soil infiltration rates at different time intervals and parameters of three well-known infiltration models including Green and Ampt (GAM), Kostiakov (KM), and modified Kostiakov (MKM) using soil readily available

characteristics. The above-mentioned models were selected based on previously published results, showing that they had the most conformity with measured infiltration data (Rahmati et al. 2016).

Several field or laboratory measured data including soil separates, K_s, D_b, D_p, *WAS*, θ_i and θ_{fs}, *OC*, and *EC* were used as input variables to develop PTFs. Soil infiltration rates were also measured in different points of the study area. In order to develop PTFs, we initially examined the correlation coefficients between the investigated parameters. Results revealed that there were significant and high correlation coefficients in most cases (Tables 3-6) which were promising to find PTFs that are more applicable. According to the very complicated process of measuring infiltration rate and in order to more precisely predict the investigated parameters, we normalized all data to prevent different dimensions' effects on PTFs development.

Applying ground measured data, we developed 25 PTFs (Table 8) to predict the investigated parameters including soil infiltration rates at different time intervals (0.5 to 45 minutes) and parameters of three infiltration models including GAM (K_a and *b*), KM (*a* and b), and MKM (*a*, b, and i_c). According to the E criteria, the developed PTFs showed high accuracies to predict infiltration rates at different time intervals having E of 0.719 to 0.964 through training data set. In addition to E, the PTFs showed also high accuracies based on ER criteria showing ER of 13 to 36 %. The developed PTFs also showed high accuracies among test data set showing E of 0.553 to 0.972 and ER of 14 to 42%. However, excluding the developed PTFs for infiltration rates at 3 and 3.5 minutes resulted in much better accuracies with E of 0.729 to 0.965 and ER of 14 to 39 % nearly close to those of the training data set. Assessing the regression coefficients revealed that K_s, D_b, θ_{fs}, θ_i, CC, and Sa were the most recurrent input variables in the developed PTFs. However, WAS, Si, OC, and D_p were other soil characteristics which were included in some cases.

The developed PTFs to predict the parameters of infiltration model also showed relatively high accuracies. According to the training data set, parameters i_c of the GAM, *a* of KM, and i_c of MKM with the respective E of 0.885, 0.948, and 0.958 and with respective ER of 22, 15, and 14 % were predicted with the highest accuracies. While parameter b of KM and MKM showed the worst accuracies with the respective E of 0.222 and 0.264 and with respective ER of 30 and 27 %. Excluding parameter b of KM and MKM and parameter *a* of MKM, the developed PTFs also showed acceptable accuracies via test data set with E of higher than 0.712.

According to the Pearson correlation coefficients between the investigated parameters and soil readily available characteristics (Table 3 and 4), soil K_s was the most effective input variable in all developed PTFs. However, soil separates, bulk density, antecedent soil moisture, and *OC* were the other major soil characteristics, which were included in nearly all cases. As outlined above, parameter *b* of the KM and MKM models showed the worst accuracy among all employed PTFs. In line with our results, Karimi (2010) also developed several PTFs to predict parameters of several infiltration models using soil readily available characteristics. Their results also revealed that developed PTFs had very low accuracies to predict parameter b of KM model showing R^2 of 0.13. It seems that linking parameter b of the KM and MKM models is much complicated, and we may need to include many other soil characteristics in PTFs development. The results by Karimi (2010) showed that the most accurate PTF was the one for the parameter S of the Suitzenderber model showing R^2 of 0.82. Mahdian et al. (2009) also developed several PTFs to predict cumulative performance of 585 infiltration measurements besides determining several soil physical properties. Their results showed that there were no significant PTF to predict cumulative infiltration.

Focusing on readily-availability of the input data to develop PTFs, remote sensing

data are among the valuable multidisciplinary sources of data that most researchers in all branches have concern about it. The applicability of the remote sensing data has been tested by soil scientists (Sidike et al. 2014, Gorji et al. 2015, Rahmati et al. 2015, 2016, Scudiero et al. 2015, He et al. 2016, Yee et al. 2016, Rahmati and Hamzehpour 2017), we tested this application for assessing the soil infiltration, as well. Therefore, we attempted at linking different parameters of soil infiltration directly to surface soil reflectance of ETM+ data or indirectly to soil properties, which are predictable by remote sensing data. In order to utilize remotely sensed data to estimate the different parameters of soil infiltration, we linked soil infiltration rates at different time intervals (0.5 to 45 minutes) to surface soil reflectance form ETM+ data. Although there were significant correlations between soil infiltration rates and surface reflectance of band 4 of ETM+ data, we could not develop a robust PTF to predict infiltration rates using surface reflectance. In order to provide an indirect way of utilizing remote sensing data in infiltration rates prediction, we also linked soil infiltration rates at different time intervals to soil properties. For this, Table 10 reports the 18 PTFs developed to predict soil infiltration rates at different time intervals having E values of 0.409 to 0.692 for the training data set. Excluding the developed PTFs for infiltration rates at time intervals 1 and 6 minutes, PTFs showed acceptable accuracies through test data set (with E of 0.409 to 0.739), as well. The obtained results reveal that although direct linkage between soil infiltration parameters to remotely sensed data seems complicated; one could use it in infiltration parameters prediction in an indirect mode. However, we assume that researchers may need to conduct more investigation for more details especially in bare soil.

Several researchers have discussed PTFs applications for prediction of soil infiltration rates at different time intervals. For example, Dashtaki et al. (2010) developed several PTFs to predict cumulative infiltration at different time intervals using soils readily available data. They reported that the applied PTFs underestimated cumulative infiltrations. Arshad et al. (2010) also developed some PTFs to predict infiltration rate using soil readily available characteristics and linear regression and artificial neural network (ANN) methods. They showed that PTFs developed by linear regression and ANN methods led to errors of 52 and 118 cm per day, respectively. Haghighi et al. (2010) applying PTFs to estimate final infiltration rate using three most applied infiltration models including MKM, Philip and the Horton models showed that the Horton model provided the best estimate of the final infiltration rate. Kashi et al. (2014) applying PTFs to predict soil infiltration rate revealed that EC and bulk density were respectively the most and the least important predictors in soil infiltration prediction.

We applied the same procedure to model the parameters of three well-known infiltration models including GAM, KM, and MKM equation using soil properties, which are predictable by remote sensing. For this, seven PTFs were developed (Table 10) to predict parameters of GAM, KM, and MKM models. PTFs to predict parameters K_a and b of the GAM model had E of 0.542 and 0.088, while those to predict parameters α and b of KM model had E of around 0.44 and those to predict parameters α, b, and i_c of MKM model had E of 0.530, 0.042, and 0.557 through training data. The accuracy based on test data was nearly similar to those based on the training data. Similar to PTFs development using ground-measured data, some parameters of investigated infiltration models showed very weak accuracies. However, the obtained results revealed that remote sensing data might be worthy to characterize soil infiltration rate or its parameters. We may need to conduct a detailed investigation on the use of remote sensing data to map infiltration rate in large watersheds. In order to get much accurate results, we need to take into account the different modeling methodologies including artificial neural networks, kriging, and co-kriging methods.

Conclusion

The current article intended to develop several PTFs to estimate soil infiltration rate and its parameters using both field/laboratories measured and remotely-sensed data. We applied linear and nonlinear regression analysis to develop PTFs to predict infiltration and its parameters. Results showed that field/laboratory measured data provide relatively high accuracies in predicting different parameters of soil infiltration. We applied remotely-sensed data in two forms of direct (surface reflectance) and indirect (soil properties which are predictable by remotely-sensed data) to develop PTFs. Although direct application of remotely sensed data resulted in no applicable PTF, indirect application of remotely-sensed data led to several PTFs, which were able to estimate soil infiltration rate and its parameters with acceptable accuracies. Therefore, these promising results showcase a new application of remotely-sensed data to predict one of the most time consuming and costly parameters, namely soil infiltration rate.

Reference

Arshad, R., Sayad, G., Mazlum, M., Jafarnejadi, A. and Mohammadi Safarzadeh, V. 2010. Pedo-transfer functions application to estimate the infiltration rate of the soil using neural network and linear regression methods. Journal of Crop Improvement. 2(5), 55-62.

Ayoubi, S., Shahri, A. P., Karchegani, P. M. and Sahrawat, K.L. 2011. Application of artificial neural network (ANN) to predict soil organic matter using remote sensing data in two ecosystems, InTech Open Access.

Bastiaanssen, W., Menenti, M., Feddes, R. and Holtslag, A. 1998. A remote sensing surface energy balance algorithm for land (SEBAL). 1. Formulation. Journal of hydrology. 212, 198-212.

Bouma, J., 1989. Using soil survey data for quantitative land evaluation. Advances in soil science, Springer. 177-213.

Clemmens, A. 1983. Infiltration equations for border irrigation models. Conference on Advances in Infiltration. Chicago, USA.

Dane, J. and Hopmans, J.W. 2002. Water Retention and Storage. Methods of Soil Analysis: Part 4 Physical Methods. Methods of Soilan. 4, 671-797.

Dashtaki, S., Araghi, F. and Mirlatifi, M. 2010. Soil cumulative infiltration prediction using PTFs in calcareous soil. Journal of Water and Soil Conservation. 17(3), 25-44.

De Roo, A., Wesseling, C. and Ritsema, C. 1996. LISEM: A single-event physically based hydrological and soil erosion model for drainage basins. I: theory, input and output. Hydrological Processes. 10(8), 1107-1117.

Gee, G.W. and Or, D. 2002. 2.4 Particle-size analysis. Methods of soil analysis. Part 4: 255-293.

Gorji, T., Tanik, A. and Sertel, E. 2015. Soil salinity prediction, monitoring and mapping using modern technologies. Procedia Earth and Planetary Science. 15, 507-512.

Grossman, R. and Reinsch, T. 2002. 2.1 Bulk density and linear extensibility. Methods of Soil Analysis: Part 4 Physical Methods. Methods of Soilan.4, 201-228.

Guo, J., Guo, S. and Li, T. 2011. Daily runoff simulation in Poyang Lake Intervening Basin based on remote sensing data. Procedia Environmental Sciences. 10, 2740-2747.

Haghighi, F., Gorji, M., Shorafa, M., Sarmadian, F. and Mohammadi, M. 2010. Evaluation of some infiltration models and hydraulic parameters. Spanish Journal of Agricultural Research. 8(1), 210-217.

He, L., Panciera, R., Tanase, M.A., Walker, J.P. and Qin, Q. 2016. Soil Moisture Retrieval in Agricultural Fields Using Adaptive Model-Based Polarimetric Decomposition of SAR Data. IEEE Transactions on Geoscience and Remote Sensing. 54(8), 4445-4460.

Jemsi, S., Sayyad, G., Jafarnezhadi, A. and KashefiPour, S.M. 2013. Development of infiltration rate pedotransfer functions using artificial neural networks and multiple linear regressions for Khuzestan province in south of Iran. International Journal of Agriculture. 3(4), 766-777.

Karimi, A. 2010. Determination of some parameters of infiltartion models using physical and chemical characteristics of soil with an emphasis on aggregates stability indicators. Master of Science, University of Tabriz.

Kashi, H., Emamgholizadeh, S. and Ghorbani, H. 2014. Estimation of soil infiltration and cation exchange capacity based on multiple regression, ANN (RBF, MLP), and ANFIS models. Communications in Soil Science and Plant Analysis. 45(9), 1195-1213.

Mahdian, M., Oskoee, R., Kamali, K., Angoshtari, H. and Kadkhodapoor, M. 2009. Developing Pedo Transfer Functions to predict infiltration rate in flood spreading stations of Iran. Research Journal of Environmental Sciences. 3(6), 697-704.

Mao, L., Bralts, V. F., Pan, Y., Liu, H. and Lei, T. 2008. Methods for measuring soil infiltration: State of the art. International Journal of Agricultural and Biological Engineering. 1(1), 22-30.

Mao, L., Lei, T., Li, X., Liu, H., Huang, X. and Zhang, Y. 2008. A linear source method for soil infiltrability measurement and model representations. Journal of Hydrology. 353(1), 49-58.

Nelson, D. and Sommers, L.E. 1982. Total carbon, organic carbon, and organic matter. Methods of soil analysis. Part 2. Chemical and microbiological properties (methodsofsoilan2): 539-579.

Nimmo, J. R. and Perkins, K.S. 2002. 2.6 Aggregate Stability and Size Distribution. Methods of Soil Analysis: Part. 4, 317-328.

Parviz, L., Kholghi, M., Valizadeh, K., Araghenezhad, S. and Irannezhad, P. 2010. Performance evaluation of normalized difference vegetation index (NDVI) through monitoring cover condition. Geomatics Conference.

Perroux, K. and White, I. 1988. Designs for disc permeameters. Soil Science Society of America Journal. 52(5), 1205-1215.

Rahmati, M. 2016. Evaluation of ETM+ data applicability for remote sensing of the soil texture and vegetation effects on accuracy of the predictions. Journal of Water and Soil Conservation (In Persian). 23(1), 187-201.

Rahmati, M. 2017. Reliable and accurate point-based prediction of cumulative infiltration using soil readily available characteristics: a comparison between GMDH, ANN, and MLR. Journal of Hydrology, 551, 81-91.

Rahmati, M. and Hamzehpour, N. 2017. Quantitative remote sensing of soil electrical conductivity using ETM+ and ground measured data. International Journal of Remote Sensing. 38(1), 123-140.

Rahmati, M., Mohammadi-Oskooei, M., Neyshabouri, M., Fakheri-Fard, A., Ahmadi, A. and Walker, J., 2014. ETM+ data applicability for remote sensing of soil salinity in Lighvan watershed, Northwest of Iran. Current Opinion in Agriculture. 3(1), 10-20.

Rahmati, M., Neyshabouri, M. R., Mohammadi Oskooei, M., Fakheri Fard, A., Ahmadi, A. and Mousavi, S. B., 2016. Evaluating and optimizing the parameters of soil infiltration models in Lighvan watershed (Northwest of Iran). Journal of Water and Soil Conservation (In Persian) 22(6), 167-178.

Rahmati, M., Neyshabouri, M.R., Oskouei, M.M., Fakheri, A. and Ahmadi, A. 2016. Soil organic carbon prediction using remotely sensed data at Lighvan watershed, Northwest of Iran. Azarian Journal of Agriculture. 3(2), 45-49

Rahmati, M., Oskouei, M., Neyshabouri, M., Walker, J., Fakherifard, A., Ahmadi, A. and Mousavi, S. 2015. Soil moisture derivation using triangle method in the lighvan watershed, north western Iran. Journal of Soil Sience and Plant Nutrition. 15(1), 167-178.

Reynolds, W., Elrick, D., Youngs, E., Amoozegar, A., Booltink, H. and Bouma, J., 2002. 3.4 Saturated and field-saturated water flow parameters. Methods of Soil Analysis. 4, 797-801.

Sarmadian, F. and Taghizadeh-Mehrjardi, R. 2014. Estimation of infiltration rate and deep percolation water using feed-forward neural networks in Gorgan Province. Eurasian Journal of Soil Science. 3(1), 1-10.

Scudiero, E., Skaggs, T.H. and Corwin, D.L. 2015. Regional-scale soil salinity assessment using Landsat ETM+ canopy reflectance. Remote Sensing of Environment. 169, 335-343.

Sidike, A., Zhao, S. and Wen, Y., 2014. Estimating soil salinity in Pingluo County of China using QuickBird data and soil reflectance spectra. International Journal of Applied Earth Observation and Geoinformation. 26: 156-175.

Yee, M.S., Walker, J.P., Monerris, A., Rüdiger, C. and Jackson, T.J. 2016. On the identification of representative in situ soil moisture monitoring stations for the validation of SMAP soil moisture products in Australia. Journal of Hydrology. 537, 367-381.